

H. Scheller
G. Fleischer
J. Kärger

Restricted self-diffusion in an aqueous solution of poly(ethylene oxide) poly(propylene oxide) poly(ethylene oxide) triblock copolymer

Received: 28 October 1996
Accepted: 21 March 1997

H. Scheller (✉) · G. Fleischer
J. Kärger
Fakultät für Physik und Geowissenschaften
der Universität Leipzig
Linnéstraße 5
04103 Leipzig, Germany

Abstract The self-diffusion behavior of a triblock copolymer (PEO-*b*-PPO-*b*-PEO) in an aqueous solution of 20% (m/m) was investigated during a temperature-induced phase transition from liquid to gel state using pulsed field gradient NMR and static light scattering. The measured self-diffusivity shows a strong dependence on the observation time in the gel phase indicating the existence of diffusion barriers in the size range of about 0.6 μm .

Additional static light-scattering measurements show a structure in the

same size range of several hundred nanometers, which is far above molecular or micellar sizes and thus, has to be caused by larger clusters.

The similarity in the space scales suggests that the restriction of molecular propagation is correlated with the grain boundaries between the domains of the poly-crystalline structure formed by the arranged micelles.

Key words Copolymers – restricted self-diffusion – interfaces – pulsed field gradient NMR – static light scattering

Introduction

Due to their amphiphilic character, block-copolymers containing poly(ethylene oxide) (PEO) and poly(propylene oxide) (PPO) show many interesting properties. PEO-PPO-PEO triblock copolymers are widely investigated using different experimental techniques. Many experiments focus on the micelle formation of these molecules in aqueous solution [1–3].

The poorly water soluble PPO-block is screened from the surrounding liquid by the PEO blocks. On increasing temperature, the molecules organize themselves in micelles which consist of a core of PPO-segments and a corona of the water soluble PEO blocks. If the concentration is larger than a critical value, a clear gel is formed. At this concentration the micelles fill the volume of the solution completely.

In fluid and fluid containing systems many intrinsic properties can be investigated by observing the irregular motion of the individual molecules (the so-called “Brownian motion”). This motion may be influenced by interfaces which are formed by both internal and external structures.

Many experimental techniques can be used to study molecular transport. The methods based on nuclear magnetic resonance (NMR) are of special interest, because these methods are non-invasive and can be used in equilibrium [4, 5]. NMR allows the observation of individual molecules without any interference with the processes and the microdynamics within the sample [6].

In this paper, we present results of our investigations of the self-diffusivity of the triblock-copolymer F88 in water below and above the gelling temperature. Whereas many investigations focus on the micellization and the properties of micelles and unimers, only very little is known about the properties of the gel state.

In the gel state we observed restricted diffusion at a space scale which is much larger than any size, which can be correlated to the unimers or micelles. For this reason static light-scattering experiments were carried out additionally to elucidate the structure of the gel.

Theory

Fundamentals of PFG NMR

To investigate molecular motion it is necessary to observe the system at different moments. For this purpose PFG (pulsed field gradient) NMR is a well-established technique, allowing the observation of molecular displacements over the space scales from below 100 nm up to several micrometers. PFG NMR monitors the motion of the ensemble of the investigated nuclei in the system. The real species which diffuse have to be known either from the chemistry of the system or have to be identified from the behavior of the measured echo attenuation.

Using an appropriate rf-pulse ($\pi/2$ -pulse) the magnetization of spins in a constant magnetic field \mathbf{B} turns from its equilibrium direction parallel to the magnetic field into the plane perpendicular to \mathbf{B} . Since a residual inhomogeneity of the magnetic field cannot be excluded, the magnetization will decay after the $\pi/2$ -pulse. Application of a π -pulse after a time interval τ refocuses the spins at time 2τ , which is known as the "primary spin-echo". In PFG NMR, the constant magnetic field is superimposed twice over the time interval δ by the additional inhomogeneous field

$$\mathbf{B}_{add} = g\mathbf{r}, \quad (1)$$

the so-called field gradient pulses. They affect the positions of the individual spins which are marked by their precessional phases. If the molecules move in the time interval t between the two gradient pulses, the refocussing will be incomplete, because their phases are different. Therefore, the spin-echo is attenuated and is dependent on the distance the molecules have moved.

Rigorous treatment of the signal attenuation in the narrow pulse approximation ($\delta \ll t$) gives the dependence of the signal on the applied gradient [7]

$$\Psi = \exp \left[-(\gamma \delta g)^2 \frac{\langle z^2 \rangle}{2} \right], \quad (2)$$

where z is the observed direction of motion which is identical to the direction of the field gradient.

Molecular motion under the influence of interfaces

The mean-square displacement in z -direction can be related to the more common self-diffusion coefficient D by the well-known Einstein relation

$$\langle z^2(t) \rangle = 2Dt. \quad (3)$$

Using this relation, the signal attenuation in a PFG NMR experiment (Eq. (2)) becomes

$$\Psi = \exp [- (\gamma \delta g)^2 Dt]. \quad (4)$$

Einstein's relation is strictly fulfilled for the motion of free molecules within an infinitely extended, homogeneous medium. In the other limiting case of completely restricted diffusion, molecules are confined within certain regions. Also in this case, the PFG NMR spin echo attenuation may be represented in the form of Eq. (4) [7] with the understanding that now the diffusivity as introduced by Eq. (3) is but an apparent one. It is thus, found to decrease with increasing observation time following a relation of the type

$$D_{app} \equiv \frac{\langle z^2 \rangle}{2t} = c \cdot t^{-1} \quad (5)$$

with $\langle z^2 \rangle = \text{const.}$

The resulting value for the quantity c allows the determination of a characteristic length of the confinement, if the confining structure is known [7].

In any intermediate case, we measure a time-dependent apparent self-diffusion coefficient with an exponent between 0 and -1 .

To extend the range of observation times we applied the stimulated echo pulse sequence [4–6]. Instead of a π -pulse, two $\pi/2$ -pulses are applied at times t_1 and t_2 after the first one. By using the stimulated echo, the NMR signal is reduced only by the longitudinal relaxation, which in polymer systems is generally slower than the transverse relaxation controlling the primary spin echo experiment.

Light scattering

We used the Rayleigh–Debye approximation [8] to investigate the size of the scattering particles. In this approximation the scattering of light of wavelength λ , which is polarized perpendicular to the scattering plane, on isotropic spheres with radius R [8] can be calculated if both the relative indices of refraction ($m = n_{scat}/n_{med}$) are close to 1 ($m - 1 \ll 1$) and the optical path length inside and outside the scattering entity does not differ too much ($2kR(m - 1) \ll 1$), to

$$\frac{I(\vartheta, R)}{I_0} = \frac{R^2}{9r^2} (kR)^4 m^2 \left\{ \frac{3}{(qR)^3} [\sin(qR) - qR \cos(qR)] \right\}^2, \quad (6)$$

where $k = 2\pi n_{\text{med}}/\lambda$ is the wave vector of the incident light and $q = 2k \sin(\vartheta/2)$ is the scattering wave vector.

The scattering of a particle collection with size distribution $v(R)$ and a scattering function $I(\vartheta, R)$ can be calculated for any scattering angle ϑ_j [9]

$$I_j = I_{\text{scat}}(\vartheta_j) = \int_0^{\infty} I(\vartheta_j, R) \frac{v(R)}{(4\pi/3)R^3} dR, \quad (7)$$

where $v(R)dR$ is the total volume of the particles within the radius interval between R and $R + dR$, thus $v(R)/(4\pi/3)R^3$ is their number.

To get an approximation for the distribution $v(R)$, the radius range from R_{min} to R_{max} is subdivided in n equally spaced intervals. In each interval the distribution function is replaced by a constant value v_i . Equation (7) then simplifies to

$$I_j = \sum_{i=1}^n v_i I_{i,j} \quad \text{with} \quad I_{i,j} = \int_{R_i}^{R_{i+1}} \frac{1}{(4\pi/3)R^3} I(\vartheta_j, R) dR. \quad (8)$$

The parameters v_i describe the total volume of the particles in the i th size interval.

The solution of this linear inhomogeneous system of equations yields an approximation for the true particle size distribution. The index j in Eq. (8), which ranges from 1 to J , denotes the measured intensity values at fixed scattering angles ϑ_j ; the index i , ranging from 1 to n symbolizes the size intervals. Because the number of size intervals is smaller than the number of measured data points, an exact solution of Eq. (8) is impossible. The optimal fit parameters are calculated using the singular-value-decomposition method, which satisfies the least-squares condition. For mathematical details of the method see Ref. [10].

Experimental setup

The spectrometer FEGRIS 400

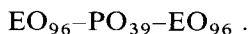
The measurements are performed at the homebuilt PFG NMR spectrometer FEGRIS (Feldgradientenimpulsspektrometer) 400 in the field of a 9.4 T superconducting magnet at a resonance frequency of 400 MHz. The maximum field gradient is 24 T/m. To be sure that the strong gradient pulses do not affect the sample, it is placed in the probe head without mechanical contact [11]. The observation times can be varied from 1 to 640 ms, the duration of the gradient pulses ranges from 100 μ s to 2 ms. To get reasonable attenuation of the spin echo, the gradient pulses in our experiments had a width of 0.85 ms. For observation times less than 8 ms the Hahn echo, above 8 ms the stimulated echo was used to determine the apparent diffusivity.

Light-scattering apparatus

To get information about internal structures in the samples, differential light-scattering measurements were performed using the light-scattering equipment at the ZAE laboratory in Würzburg [12]. The sample is illuminated by a He-Ne laser beam at a wavelength of 633 nm, which is polarized perpendicular to the scattering plane. The scattered intensity is measured as a function of the scattering angle. The sample can be heated to the desired temperature by air flow.

Samples

F88 is a type ABA triblock copolymer consisting of ethylene oxide [EO] $\text{CH}_2\text{--CH}_2\text{--O}$ and propylene oxide [PO] $\text{CH}_2\text{--CH}(\text{CH}_3)\text{--O}$ with the average composition



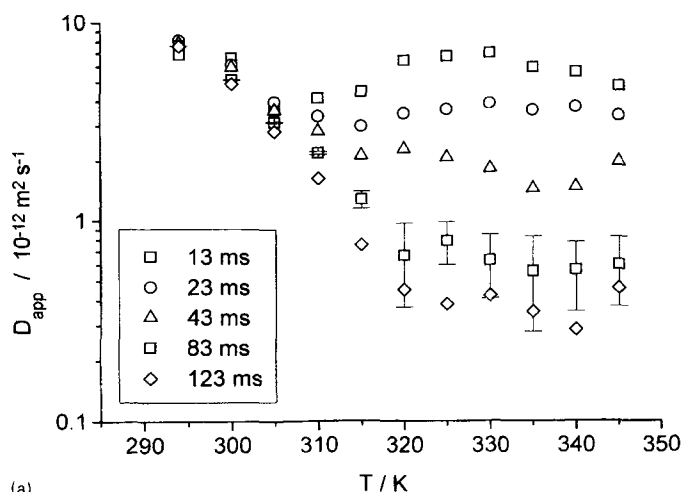
Aqueous solutions of F88 form micelles at temperatures of about 30 °C, whereas the phase transition temperature slightly depends on the concentration. If the concentration is larger than 20% (m/m), the micelles form a cubic crystal [3]. This leads macroscopically to the formation of a clear gel. This phenomenon is known as "inverse melting" [3].

To investigate the diffusion properties of the polymer it is dissolved in deuterated water, thus the solvent molecules are "invisible" to the ^1H PFG NMR measurement. Because of the solubility properties of PEO and PPO, cooling of the sample is very helpful to accelerate the solution process, which can extend to several weeks depending on the concentration. For the experiments, we have used F88 from BASF, Parsippany, NJ (USA) without further purification.

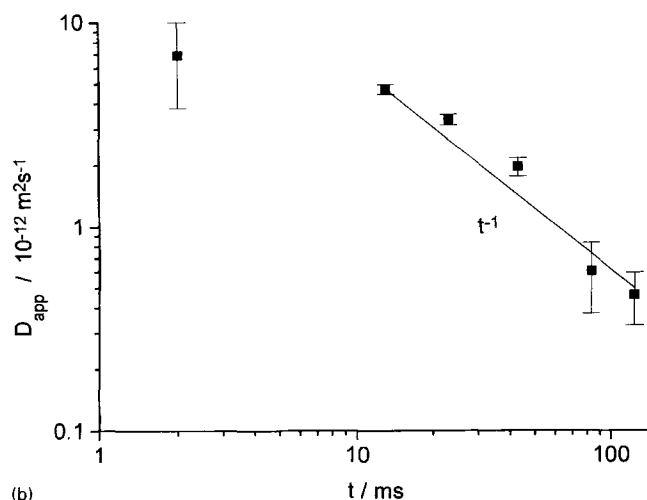
Results and discussion

We investigated the diffusion behavior of the polymer molecules in the temperature range below and above the gelation point. We used a 20% (m/m) solution, because this is nearly the least necessary amount of polymer to get gelation of the solution [3].

Figure 1a shows the measured apparent self-diffusion coefficients D_{app} of a 20% (m/m) solution as a function of temperature. At room temperature the diffusion coefficient of the solution does not depend on the observation time. The molecules move freely. On increasing temperature the motion of the molecules slows down which is typical for the formation of micelles [1]. This can be observed up to 305 K.



(a)



(b)

Fig. 1 Apparent self-diffusion coefficient D_{app} of a 20% (m/m) solution of F88 as a function of temperature for different observation times (a). D_{app} as a function of observation time at 345 K (b)

In this temperature range, the measured self-diffusion coefficient depends on the observation time only weakly, and within experimental error, only for Δ larger than 43 ms. This means, that there is a weak influence of diffusion barriers on the motion of the molecules visible even at temperatures below gelation. Further increase of the temperature then leads to a dramatic change in the self-diffusion behavior of the solution.

At temperatures above 320 K the apparent self-diffusivity depends strongly on the observation time Δ , whereas there is only a weak temperature dependence. At short observation times an increase from 305 to 325 K and a small decrease above that temperature range can be seen. This decrease may be due to a transition in the shape of the

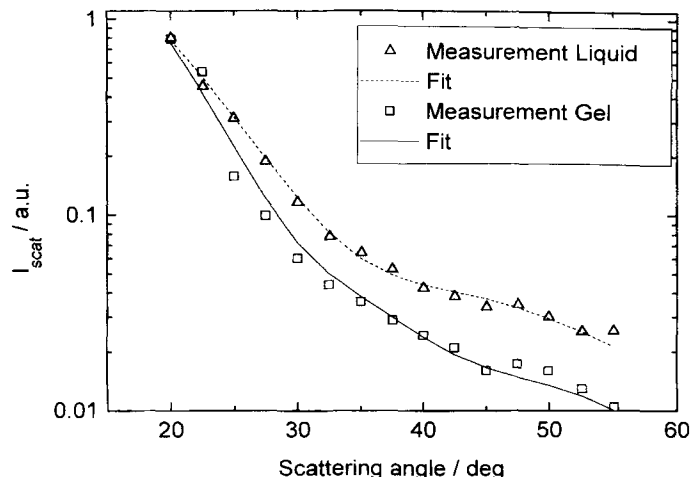


Fig. 2 Measured scattered intensity and fit curves according to Eq. (8) at room temperature (Δ , —) and at 323 K (\square , --)

micelles, which is reported for the micelles of the similar polymer P85 [13]. At larger observation times the apparent self-diffusivity is constant up to 345 K.

This is the typical behavior for molecules diffusing in confined space. The dependence of D on Δ is depicted in Fig. 1b for 345 K. Obviously, the motion of the molecules is completely restricted (Eq. (5)) for observation times larger than 10 ms. Using Eq. (3), the apparent self-diffusion coefficient is found to correspond to a mean-square displacement $\langle z^2 \rangle^{1/2}$ of 0.35 μm . Under the assumption that the confining regions are of spherical shape, the corresponding radius a can be calculated [7] via

$$\frac{\langle z^2 \rangle}{2} = \frac{a^2}{5} \quad (9)$$

to be about 0.55 μm . This value is significantly larger than any molecular or micellar length. Thus, the diffusion barriers have to be the grain boundaries of the polycrystalline structure, which is formed at the gelation and reported by neutron scattering experiments [14].

To confirm these findings and to get more information about the diffusion barriers static light scattering experiments were performed.

Figure 2 shows the measured light scattering distribution and the fit curves below and above gelation temperature. Both curves are strongly forward-peaked indicating the existence of large scattering centers. However, the scattering distribution of the liquid at angles larger than 40° is more isotropic than in the gel state. This reveals that smaller particles which exist at lower temperatures, disappear when the gel is formed.

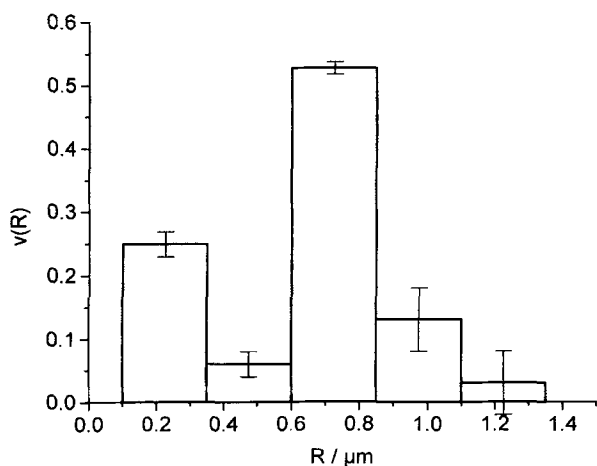


Fig. 3 Relative volume $v(R)$ of scattering particles with radius R of the liquid state of the solution corresponding to the fit curve of Fig. 2

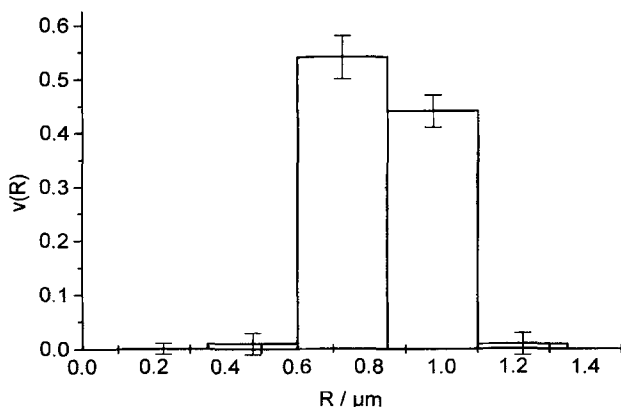


Fig. 4 Relative volume $v(R)$ of scattering particles with radius R of the gel state of the solution corresponding to the fit curve of Fig. 2

As in the NMR experiments, above gelation, no change in the angular distribution of the scattered light could be observed at further temperature increase in the gel state.

As a first approximation to get information about the size of the scattering domains we used the Rayleigh–Debye approximation for spheres, which may be justified by the observations that the formed gel is clear, indicating, that there are no big differences in the index of refraction and by the size range, which results from the NMR measurements. Particle sizing was done using the histogram fit method described in Light Scattering Section.

It should be emphasized at this point that the entities which cause the light scattering cannot be the unimers or

the micelles. If they would cause the light scattering, the distribution of the scattered light has to be isotropic because of the small size of those entities.

Taking the results of the NMR measurements into account, we subdivided the size range from $0.1 \mu\text{m}$ up to $1.35 \mu\text{m}$ into 5 equally sized intervals. A fit according to Eq. (8) was performed yielding the lines shown in Fig. 2.

Figures 3 and 4 represent the size distributions of the liquid and the gel state of the solution resulting from the fit procedure. Both results show a maximum at about $0.7 \mu\text{m}$. This may be due to the fact that also at room temperature there exists a prearrangement of the micelles to clusters already in the liquid state. These prearranged clusters then form the domains which are formed during gelation and may be the reason for the weak diffusion restriction which was measured at temperatures near but below the gelation point. In the gel state, however, the smaller particles or domains disappear, whereas the size distribution becomes peaked at about $0.8 \mu\text{m}$.

Because of the mathematical method, the total number of intervals is limited. For too many (and hence for too small) intervals the fitting procedure also leads to negative values for the parameters, which are physically senseless. The border values for the fit procedure have been determined by test calculations where the χ^2 -criterion was taken into account.

The similarity of the obtained characteristic length scales suggests that both the PFG NMR and the light-scattering measurements reveal the same structure. This structure is significantly larger than the micellar indicating the formation of a hyperstructure in the form of a polycrystalline micellar crystal. Such a polycrystalline structure in the gel state of aqueous solutions of PEO–PPO–PEO triblock copolymer was found by Mortensen [15] from small-angle neutron scattering experiments. We assume that the diffusion restriction is caused by the “grains” of individual crystalline domains. Such a transport barrier was also observed in lamellar-ordered polystyrene/polyisoprene diblock copolymers by field gradient NMR [16].

At the grain boundaries the local concentration of polymer is smaller than in the core, which causes the light scattering. Also the composition may be different, what may as well lead to a difference in the refractive index. The deviation in the absolute values of the results of NMR and LS may result from different reasons. Most probably the assumption of spherical domains is a crude approximation. Moreover, the heating rate during the measurements, the geometry of the sample and its history, which cannot be identical in these two different types of measurement, are most likely to affect the formation of the crystalline domains. It has also to be noted, that PFG NMR

experiments and light scattering have a very different averaging behavior with respect to the size distribution of the measured "particles".

Conclusion and outlook

The existence of mesoscopic structures in the gel phase of aqueous solutions of triblock-copolymer F88 is revealed by the joint application of PFG NMR and static light scattering. The mesoscopic structures are explained by the

formation of crystalline domains which act as both transport barriers and light-scattering centers.

More detailed studies of the influence of concentration, temperature and heating rate on the formation of the mesoscopic structures are in progress.

Acknowledgments Financial support by the "Deutsche Forschungsgemeinschaft" (SFB294 "Moleküle in Wechselwirkung mit Grenzflächen" and Graduiertenkolleg "Physikalische Chemie der Grenzflächen") is gratefully acknowledged.

We are indebted to Prof. Dr. Fricke and Dr. Werner Körner (ZAE Bayern-Bavarian Center for Applied Energy Research) for the light-scattering measurements.

References

1. Fleischer G (1993) *J Phys Chem* 97:517-521
2. Glatter O, Scherf G, Schillén K, Brown W (1994) *Macromolecules* 27:6046-6054
3. Mortensen K, Schwahn D, Janssen S (1993) *Phys Rev Lett* 71:1728-1731
4. Kärger J, Ruthven DM (1992) *Diffusion in Zeolites and Other Microporous Solids*, Wiley, New York
5. Callaghan PT (1993) *Principles of Nuclear Magnetic Resonance Microscopy*, Oxford University Press, Oxford
6. Kärger J, Fleischer G (1994) *Trends Anal Chem* 13:145-157
7. Kärger J, Pfeifer H, Heink W (1988) *Adv Magn Res* 12:1-89
8. Kerker M (1969) *The Scattering of Light*, Academic Press, New York
9. Dave JV (1971) *Appl Opt* 10:9
10. Press W, Flannery B, Teukolsky S, Vetterling W (1989) *Numerical Recipes in Pascal*, Cambridge University Press, Cambridge
11. Kärger J, Bär NK, Heink W, Pfeifer H, Seiffert G (1995) *Z Naturf* 50a:186-190
12. Beck A, Körner W, Hoffmann T, Fricke J (1992) *Appl Opt* 31:3533-3539
13. Mortensen K, Pedersen JS (1993) *Macromolecules* 26:805-812
14. Mortensen K, Brown W, Nordén B (1992) *Phys Rev Lett* 68:2340-2343
15. Mortensen K (1992) *Europhys Lett* 19:599-604
16. Fleischer G, Fujara F, Stühn B (1993) *Macromolecules* 26:2340-2345